Evidence for Phanerozoic Reactivation of the Najd Fault System in AVHRR, TM, and SPOT Images of Central Arabia

Constance G. Andre
Center for Earth and Planetary Studies, Smithsonian Institution, Washington, DC 20560

ABSTRACT: SPOT stereoscopic and TM multispectral images support evidence in AVHRR thermal-IR images of a major unmapped shear zone in Phanerozoic cover rocks southeast of the ancient Najd Fault System in the Arabian Shield. This shear zone and faults of the Najd share a common alignment, orientation, and sinistral sense of movement. These similarities suggest a 200-km extension of the Najd Fault System and reactivation since it formed in the late Precambrian. Topographic and lithologic features in the TM and SPOT data along one of three faults inferred from the AVHRR data indicate sinistral offsets up to 2.5 km, *en echelon* folds and secondary faults like those predicted by models of left-lateral strike-slip faulting. The age of the affected outcrops indicates reactivation of Najd faults in the Cretaceous, judging from TM and SPOT data or in the Tertiary, based on AVHRR data. The total length of the system visible at the surface measures 1300 km. If the Najd Fault System is extrapolated beneath sands of the Empty Quarter to faults of a similar trend in South Yemen, the shear zone would span the Arabian Plate. Furthermore, if extensions into the Arabian Sea bed and into Egypt proposed by others are considered, it would exceed 3,000 km.

INTRODUCTION

ONE APPROACH to studying transcurrent faults in inaccessible areas has three phases: (1) get an integrated view of the whole system from AVHRR (Advanced Very High Resolution Radiometer) thermal-IR space images with low spatial resolution; (2) use high-resolution TM multispectral and SPOT stereoscopic space images to refine the location and extent and determine the timing, sense of motion, and offset; and (3) select critical locations for field work to test the hypotheses evolving from Phases 1 and 2.

This paper is a report of Phase 2 of a study to test the hypothesis of Andre and Blodget (1984) that an unmapped shear zone in the Arabian platform is an extension of the Precambrian Najd Fault System and was reactivated since the Paleozoic.

The Arabian Peninsula is a small plate bounded by the Arabian Sea and Gulf of Aden on the south; the Red Sea spreading center, Gulf of Aqaba, and Dead Sea rift zone on the west; the Zagros thrust zone on the north and northeast; and the Oman obduction zone on the southeast. The net effect of the stresses is counterclockwise rotation away from Africa (Quennell, 1958). The plate is estimated to have been displaced 105 km to the north along the Dead Sea Fault: 60 km before the Miocene and 45 km since then, a rate of 0.4 to 0.6 cm per year during the last 7 to 10 million years (Freund *et al.*, 1970). The most active spreading in the Red Sea is in the south at a rate of about 1 cm per year for the last four or five million years (Gettings *et al.*, 1986).

The core of the Plate, the Arabian Shield, is exposed from the Red Sea coast to more than 500 km inland (A on Figure 1). The Shield is marked by subparallel and braided faults with orientations of N45°W to N55°W that comprise the Najd Fault System (Figure 2). The fault system is a complex set of left-lateral strike-slip faults and ductile shear zones that form a band 400 km wide with an exposed length of 1100 km (Moore and Al Shanti, 1979). Local left-lateral displacements of 2 to 25 km have been mapped along the main fault (Brown, 1972). The cumulative displacement has offset the northern part of the craton 250 km to the northwest (Stoesser and Camp, 1985). Most of the displacements along faults of the Najd occurred between 620 and 540 Ma (Stern, 1985) on four or five main strands (Moore and Al-Shanti, 1979). But, some Tertiary reactivation has been noted (Moore, 1979).

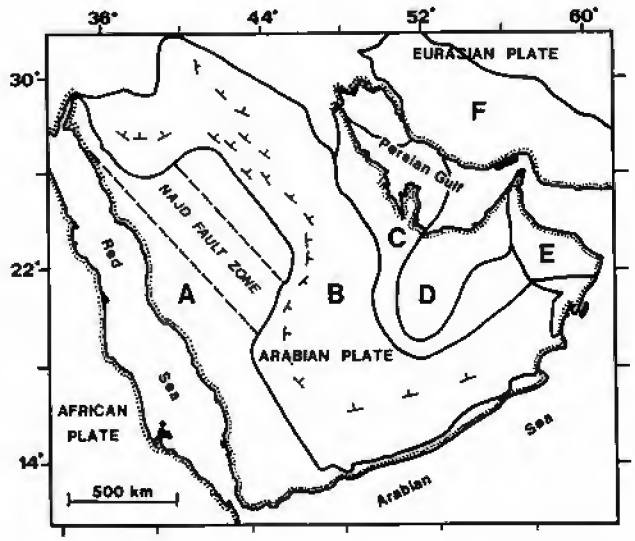

FIG. 1. Structural provinces of the Arabian Plate simplified from Powers *et al.* (1966). A, Arabian Shield; B, Interior Homocline and Hadramawt Plateau; C, Interior Platform; D, Rub al Khali Basin; E, Oman Mountains; F, Zagros Mountains; general outline of the Najd Fault System between dashed lines.

The Shield is progressively overlain to the east by Permian, Mesozoic, and Cenozoic limestones and sandstones that dip eastward at less than 3 degrees (Powers *et al.*, 1966). These sedimentary formations have a cumulative thickness of more than 2000 m and are well exposed along numerous west-facing erosional scarps (cuestas) of the Interior Homocline (B on Figure 1). These cuestas strike approximately north and extend for hundreds of kilometres. It has long been suspected that faults of the Najd extend beyond the southeast termination of the exposed Shield into Phanerozoic cover. Fault extensions have

PHOTOGRAMMETRIC ENGINEERING AND REMOTE SENSING,
Vol. 55, No. 8, August 1989, pp. 1129–1136

0099-1112/89/5508–1129$02.25/0

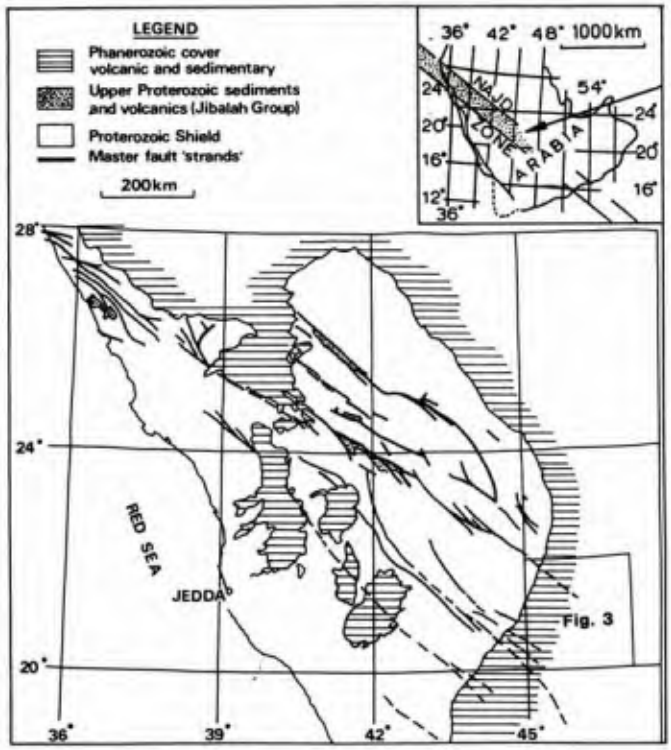

FIG. 2. Index map of the Najd fault system of the Arabian Peninsula before the Red Sea opened, and map of the main faults in this zone in the Shield (Moore, 1983). The AVHRR thermal-IR image of the southeast quadrant of the map showed faults in the Shield and three main extensions into Phanerozoic sedimentary cover east of the Shield. SPOT stereoscopic data and TM multispectral data have been used to study one of these extensions within the area marked Figure 3. It is parallel to and south of the one seen in the northwest corner of this square.

been tentatively mapped on tectonic maps of Brown (1972) and Moore (1979).

To the east of the homocline, these formations form the Rub al Khali Basin (D on Figure 1) that contains extensive sands and gravels of the Empty Quarter, where the crystalline basement is estimated to lie more han 9000 m below sea level (Brown, 1972). This deep basin has been subsiding since the Tertiary as the basement has buckled in response to collision of the Arabian and Eurasian Plates (Powers *et al.*, 1966).

PREVIOUS STUDIES

Moore (1979) compared aeromagnetic maps of the Shield to early satellite images and aerial photos of the Najd Transcurrent Fault System and concluded that it is broader and the structures more continuous at depth than indicated by faults at the surface. Within the belt of strike-slip faults, there are numerous uplifted, down-faulted, and tilted blocks that he attributes to a history of progressive unloading and uplift, primarily in the Proterozoic. Characteristics of the left-lateral fault zone he describes are similar to those seen in the TM and SPOT images. He noted both folds and Riedel shears with axial traces *en echelon* along the major faults. He attributes the fault patterns to simple shearing between rigid blocks beneath the exposed structures where the maximum principal compressive stress was oriented approximately east-west. The last reactivation was during Tertiary rifting events in the Red Sea region, he reports. He estimates that block movement along the Najd has affected the Phanerozoic cover strata for more than 100 km southeast of the edge of the Shield. Structural contours on the buried surface of the Crystalline Shield southeast of the exposed Shield, based on drill records, show discontinuities that coincide with Najd fault extensions plotted from Gemini and Apollo photographs (Brown, 1972). It will be shown that in AVHRR, TM, and SPOT data, there is surface evidence of faulting to a distance of 200 km into the Phanerozoic cover.

In Phase 1 of this study, AVHRR thermal-IR images indicated several subparallel unmapped faults that extend the trend of the Najd zone into the sedimentary cover (Andre and Blodget, 1984; Andre, 1987). They found that a color image (covering the southeast quadrant of Figure 2) combining three thermal-IR bands from day and night data shows the Najd faults in the Shield as "cool" at night, perhaps due to evaporative cooling along fault breccia seams. Pairs of day/night thermal-IR images were used to accentuate differences in physical properties of surface material, e.g., density, porosity, moisture content, fragment size, or thermal conductivity. The three thermal bands were used to separate different sedimentary rock types, thus allowing mapping of lithologic contacts and their displacements. The extension of the master Najd fault, tentatively mapped by Brown (1972) and Moore (1979), can be traced for 200 km (an additional 75 km) into the interior homocline. It crosses eight north-northeast-striking cuestas at nearly right angles (Figure 3a). The cuestas have uppermost strata that range in age from Triassic to Tertiary (Figures 3a, b, and c). Andre and Blodget (1984) suggested that Tertiary reactivation of Najd faults in the basement beneath the cover was related to tectonic activity associated with formation of the Red Sea. The TM and SPOT images used in this study cover one of three unmapped faults interpreted from low-resolution AVHRR data (Andre and Blodget, 1984). The approximate trace of this fault zone from AVHRR data is shown on a simplified geologic map (Figure 3a) of the area outlined in Figure 3c.

DATA SOURCES

The combination of TM multispectral and SPOT stereoscopic images is particularly valuable for mapping lithologic and topographic offsets of faults in areas that are difficult to access, like the central Arabian Peninsula. Each instrument provides something unique: TM bands 1, 5, 7, and 6 measure the response in visible, near-IR, and thermal-IR wavelengths. The SPOT instrument has the highest spatial resolution of the three, 10 m in the panchromatic mode, and stereoscopic coverage (Table 1). The TM and SPOT subscenes (Figure 3) cover a large segment of the fault inferred from AVHRR thermal-IR data. They are outlined and numbered on a simplified geologic map of the area (Figure 3a) that also shows a cross-section of the cuestas (Figure 3b) intersected by the inferred fault at an angle of 65° to 85°. The arid environment, sparse vegetation, and broad outcrops of Permian through Tertiary strata are optimum conditions for use of these data.

INTERPRETIVE FRAMEWORK: STRIKE-SLIP FAULT GEOMETRY

The lithologic and topographic features mapped from the TM and SPOT images are compared to the geometry of primary and secondary features of strike-slip faulting. The mechanics of strike-slip faulting have been studied in theory, in the laboratory and in the field. The theoretical geometry of a "pure shear" (e.g., Moody and Hill, 1956) closely matches the angles of faults and folds in laboratory models (e.g., Wilcox *et al.*, 1970); but Sylvester (1988) shows that major strike-slip fault systems, such as the Najd, are better described by the Riedel model of "simple shear." The model is drawn as a left-lateral fault system with a principal displacement zone striking N55°W (Figure 4) for comparison to the Najd fault extension. Several of the features illustrated in Figure 4 match those seen in multispectral and stereoscopic images from TM and SPOT.

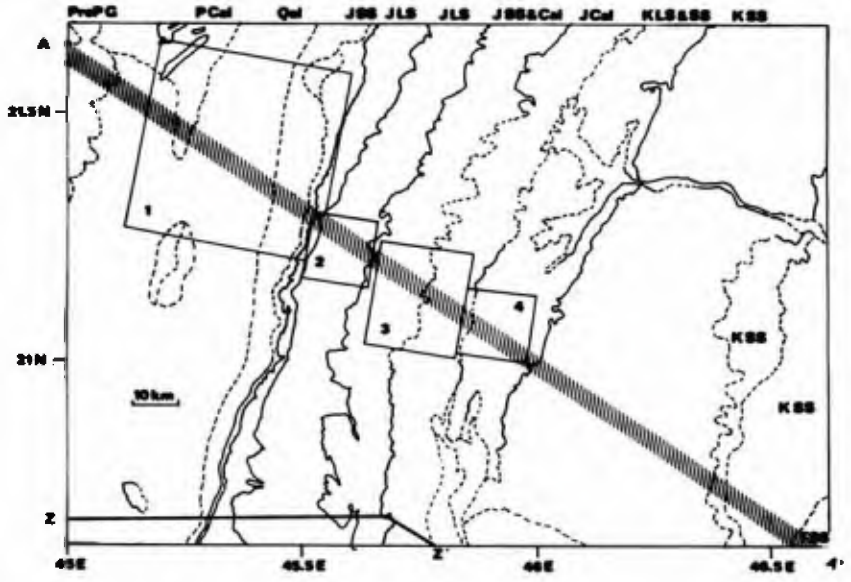

(a)

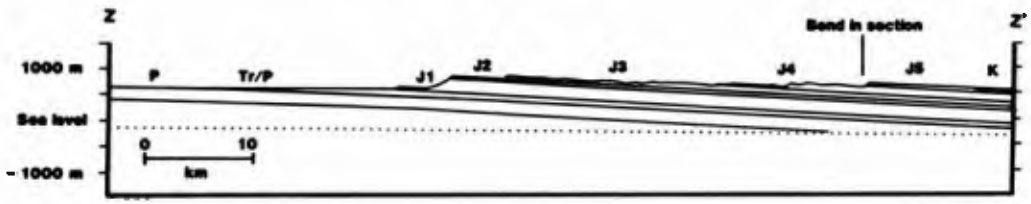

(b)

(c)

FIG. 3. (a) Satellite subscenes within the area shown in Figure 2 that are discussed in the text are outlined on a geologic map simplified from Bramkamp *et al.* (1956). AVHRR thermal-IR images include the whole area. KEY: PreP, pre-Permian; P, Permian; J, Jurassic; K, Cretaceous; T, Tertiary; Q, Quaternary; G, granite; Cal, calcareous; SS, sandstone; LS, limestone; and al, alluvium. The zone (A – A') indicates the location of one of the faults interpreted from AVHRR thermal-IR images discussed in this report. (b) Cross-section along reference line Z – Z' on Figure 3a. Vertical exageration = 5. From Bramkamp *et al.* (1956). (c) Landsat MSS mosaic (Moore, 1983) showing the location of Figure 3a.

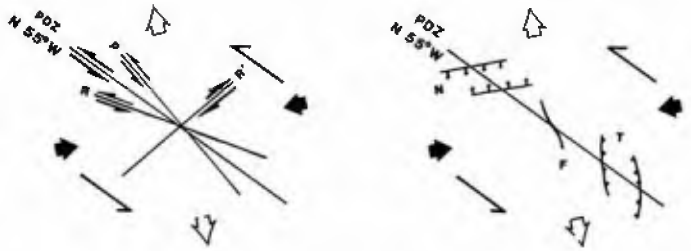

FIG. 4. Geometric relationship of faults and folds in a two-dimensional strike-slip fault system according to the Riedel model of left "simple" shear with the principal displacement zone (PDZ) oriented N55°W like the fault interpreted from TM and SPOT images. Solid arrows, axis of shortening; open arrows, axis of lengthening; R, Riedel shears; R', conjugate Riedel shears; F, *en echelon* fold; P, secondary synthetic strike-slip fault; T, thrust fault; and N, normal fault. Modified from Sylvester (1988).

TABLE 1. SATELLITE DATA USED IN THIS STUDY

	SPOT Panchromatic*	Landsat TM	NOAA AVHRR
Spatial Resolution:	10 - 13 m	30 m	1100 m
Local Solar Time:	11:15 a.m.	10:00 a.m.	3:15 a.m.
			3:15 p.m.
Date:	17 Jun 86	21 Feb 85	16 Sep 82
	21 Jun 86		17 Sep 82
Spectral Bands used (in microns)	0.51- 0.73	0.45- 0.52	3.55- 3.93
		0.63- 0.69	10.30-11.30
		1.55- 1.75	11.50-12.50
		10.4 -12.5**	
		2.08- 2.35	

* SPOT incidence angles for 2 stereopairs: 23° & 21°; 27° & 17°
** 120 m spatial resolution

REGIONAL EVIDENCE OF FAULT BLOCKS

ALIGNED BENDS IN PARALLEL CUESTA SCARPS

Reference line A–A' (Figure 3) has an orientation of N55°W and marks the general location of one fault inferred from the AVHRR thermal-IR image. It is about 200 km long and intersects numerous parallel cuestas of the Interior Homocline (B on Figure 1). At the line of intersection, the trends of the cuesta scarps change. North of the fault, the scarps trend farther east of north than those south of it. The shift is from about N15° – 25°E for the southern part of the scarps to N25° – 30°E for the northern part. Assuming a common strike initially, this change can indicate convergence or divergence along a fracture between fault blocks. Other changes in strike of the scarps appear to separate the homocline into poorly defined segments and have been related to possible flexing of the basement (Powers *et al.*, 1966), yet there is no record of faulting in the interior of the Peninsula.

OFFSETS OF SCARPS

In regional TM and SPOT scenes, there are numerous lateral "stair steps" at the intersection of the fault and the parallel cuesta scarps (individually shown later in Plates 1a, 2a, 3a and 4a). The aligned displacements are interpreted as left-lateral offsets. These steps to the northwest immediately north of the fault are not likely to be due to differential erosion because the rock types north and south of it are homogeneous. If attributed to tectonics, the distance along the fault where evidence of sinistral displacement can be found is about 65 km. The orientation of the steps, their alignment along the fault, and sense of movement are characteristic of faults in the Najd System.

DRAINAGE DIVIDE

The bedding planes of the Interior Homocline (and the back sides of cuestas) dip one or two degrees to the east (Figure 3b). Such slopes should produce a subdendritic to subparallel drainage pattern (Phillips and Schumm, 1987). Locally, drainage is controlled by west-facing scarps. A map of the primary drainage routes (Figure 5) indicates that the drainage network has been tectonically modified; a change in the direction of drainage occurs in a narrow zone along line A – A'. South of the zone, the drainage direction is toward the east down dip slopes and then south. North of the zone, drainage is toward the north and east. This drainage divide extends more than 100 km, from the Shield to Cretaceous outcrops, supporting the suggestion that it separates two fault blocks. Counterclockwise rotation of the southern block away from the northern block along a horizontal axis defined by A – A' is one possible explanation for the change in slope. A slope change of only one or two degrees can alter

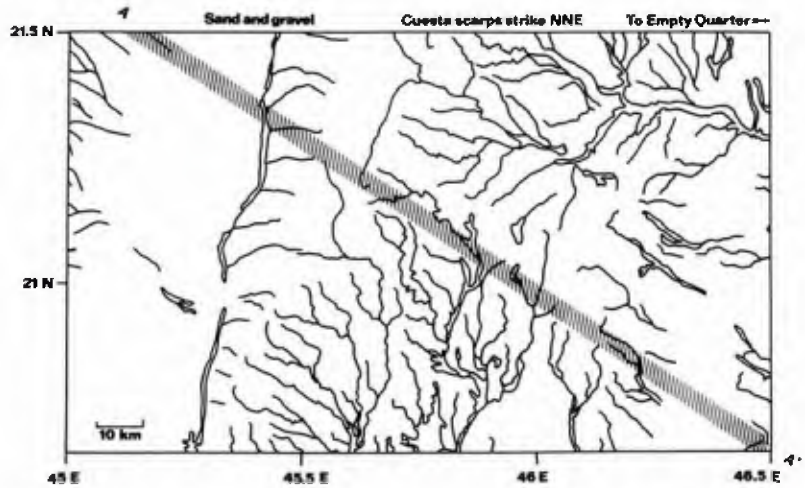

FIG. 5. Primary wadi channels in Phanerozoic cover rocks. The change in drainage direction in a zone along A – A' is perhaps due to tilting of the strata away from the boundary between two fault blocks.

TABLE 2. KEY TO INTERPRETIVE SKETCHES

Apparent fault	:	A – A'
Wadi	:	
Area rich in iron oxide	:	
Erosonal debris	:	
Ridge	:	
Cuesta scarp	:	
indistinct one	:	
Strike-slip fault	:	
Vertical displacement (side up or down)	:	U / D
Syncline	:	
Anticline	:	
Thrust fault sawteeth on upthrown side	:	

the drainage pattern (Phillips and Schumm, 1987). In summary, aligned sinistral displacement of the cuesta scarps, consistent shifts in their strikes, and a drainage divide within a narrow zone centered on A – A′ suggest a strike-slip fault with convergent/divergent and rotational components of faulting between two blocks.

Local Evidence of Faulting

Outcrops of successively younger strata from west to east (Figure 3a) were studied in TM and SPOT subscenes to refine the location of the inferred fault between the two blocks, to map associated secondary folds and faults, and to estimate the time of reactivation. The TM subscenes are discussed together with interpretive sketches showing pertinent features in the images. A key in given in Table 2 for symbols used in the sketches.

Structural and Erosional Features in Permian, Triassic, and Lower-Jurassic Outcrops

Local surface structure and lithologic units interpreted from a TM image indicate that a northwest-trending fault crosses Permian and Triassic strata (Plate 1a, from Subscene 1 on Figure 3a). The image was designed to show areas of high iron oxide concentration in red by combining only Bands 1 and 3. Band 1, (blue-green) has low values relative to Band 3, (red) for ferric iron minerals (American Society of Photogrammetry, 1983).

The sketch in Plate 1b shows the location and interpretation of features in the image that indicate displacement along a fault. From west to east, they are (1) a straight wadi, about 30 km long, that originates in the Shield west of the image; (2) sinistral offsets of a ridge (white) on the west side of the image and of two cuesta scarps on the east side (dark); and (3) a dip-slip component suggested by the abrupt termination at the fault of two erosional units at the base of the local gravels on the east side of the image, i.e., a broad sediment-filled drainage area (white) and the adjacent iron-rich unit (dark red/brown) in the center of the image. Neither deposit is visible south of the fault. The red unit in the image (high Fe^{3+}) can be traced eastward along wadis to Jurassic sandstones (dark) described as buff, brown and red (Bramkamp *et al.*, 1956), consistent with Fe^{3+} enrichment. If these sandstones are the source of the high concentrations of iron oxide, more active erosion and higher elevations north of the fault are suggested, because the lithology is homogenous north and south of it. A difference in elevation is consistent with the explanation for the regional drainage divide, i.e., differential tilting of the fault blocks away from the fault zone.

Structural Features in Mid-Jurassic Outcrops

The TM subscene to the east of Plate 1a shows primary and secondary structures in mid-Jurassic limestones and sandstones that are typical of left-lateral faulting (Plate 2a from Subscene 2 on Figure 3). The jog in the strike of the scarp (red) in the northwest corner of the scene (an enlargement of the one on the east side of Plate 1a) suggests a sinstral offset of the Jurassic limestone scarp by about 2.5 km (Plate 2b). Generally, the paths of wadis (green) are structurally controlled by small scarps of bedding planes within the cuestas and erosion. But, tectonic influence is also suggested by a change in drainage direction near A – A′ and disruption of drainage, i.e., the green lines at the northeast end of the fault. In the center of the image, curved drainage lines below the fault define a wedge shape. The axis of the wedge (anticline in Plate 2b) runs along the top of an arch seen in a SPOT stereopair. Older strata (dark blue) that underlie the cap rock (red) are exposed along the axis at the west end, typical of anticlinal forms in layered material. The axis trends northwest to form a 12° angle with the fault, close to the angle predicted for *en echelon* (drag) folds (Figure 4). The apex of the wedge points west, opposite to the direction of relative displacement proposed for the fault block it occupies, a characteristic of left-lateral strike-slip faulting. The anticline is asymetrical with tighter folds on the side closest to the apparent fault, like *en echelon* folds along the San Andreas fault (Harding, 1976). The 7-km long wadi to the south is interpreted as the complementary syncline. It forms a trough for the wadi channel (Plates 2a and 2b). The morphology, geometry, and scale of the anticline/syncline pair form a mirror image of those found along the right-lateral San Andreas Fault (Harding, 1976).

Segmented units outlined by drainage routes near the fault (center of Plate 2a) resemble elongate lenses seen in laboratory simulations of left-lateral faults. These lenses form following peak resistance to primary stress when passive material is isolated between the principal displacement shears as these shears begin to replace the *en echelon* synthetic shears (Tchalenko, 1970), R on Figure 4. These lenses have also been seen in field studies of left-lateral faulting on the Tibetan Plateau (Armijo *et al.*, 1986).

Topographic Features in Upper-Jurassic Outcrops

No evidence of faulting is seen in the two upper-Jurassic formations (Subset 3, Figure 3) along A – A′ in TM visible, near-IR, or thermal-IR data. However, in a higher resolution SPOT stereopair (not shown), the fault is discontinuously marked by steep topographic relief and straight narrow wadi channels that cannot be resolved in the Thematic Mapper images. Fault traces are natural channels for wadis and erode faster than adjacent bedrock.

Lithologic Features in Upper-Jurassic and Lower-Cretaceous Outcrops

When adjacent broad scarps of limestone and sandstone are laterally displaced normal to their strikes, the offset can be detected in a TM near-IR image combining bands 5 and 7 (e.g., Plate 3a). The lower spectral reflectance in band 7 relative to band 5 for calcareous rock types (e.g., limestone) relative to high-silica types (e.g., sandstone) accentuates the offset of the lithologic contact (American Society of Photogrammetry, 1983). Thus, a TM image has been constructed to show sandstones in red tones and limestones in blue tones (Plate 3a from Subset 4 in Figure 3a). Displacement of the northern fault block to the northwest would cause a stairstep pattern along northnortheast-trending scarps between limestones and sandstones. Within the scene, there is a calcareous outcrop on the east side (dark blue tones), a sandstone unit in the center (light and dark red/brown tones) and a limestone outcrop (blue tones) on the west side, crossed by three broad wadis (dark). Jogs in the two scarps (dark) separating these three lithologic units are aligned along the apparent fault in a stair-step pattern indicating left-lateral displacement of the northern fault block relative to the southern one by about 2.5 km (Plate 3b). The direction and degree of displacement are comparable to those in the lower Jurassic outcrop shown in Plates 2a and 2b.

SPOT stereopairs for this TM subset show that the center wadi on the west side follows the fault for a distance of more than 3 km. The stereopairs also show lower elevations south of the fault, a sign of vertical displacement of the fault blocks in addition to horizontal displacement.

Other structures associated with sinistral faulting of this Cretaceous outcrop can be seen in a SPOT subscene with higher spatial resolution (Plate 4a). Two north-south trending features within the promontory intersect the fault at angles of about 55°. The SPOT stereopair indicates that the surface between them is higher than adjacent areas. The larger deposits of detritus east of the higher area are consistent with this difference in surface elevation. A comparison with the geometry of faults and folds associated with the left-lateral faulting predicted by models of "simple" shear when the principal displacement zone is N55°W

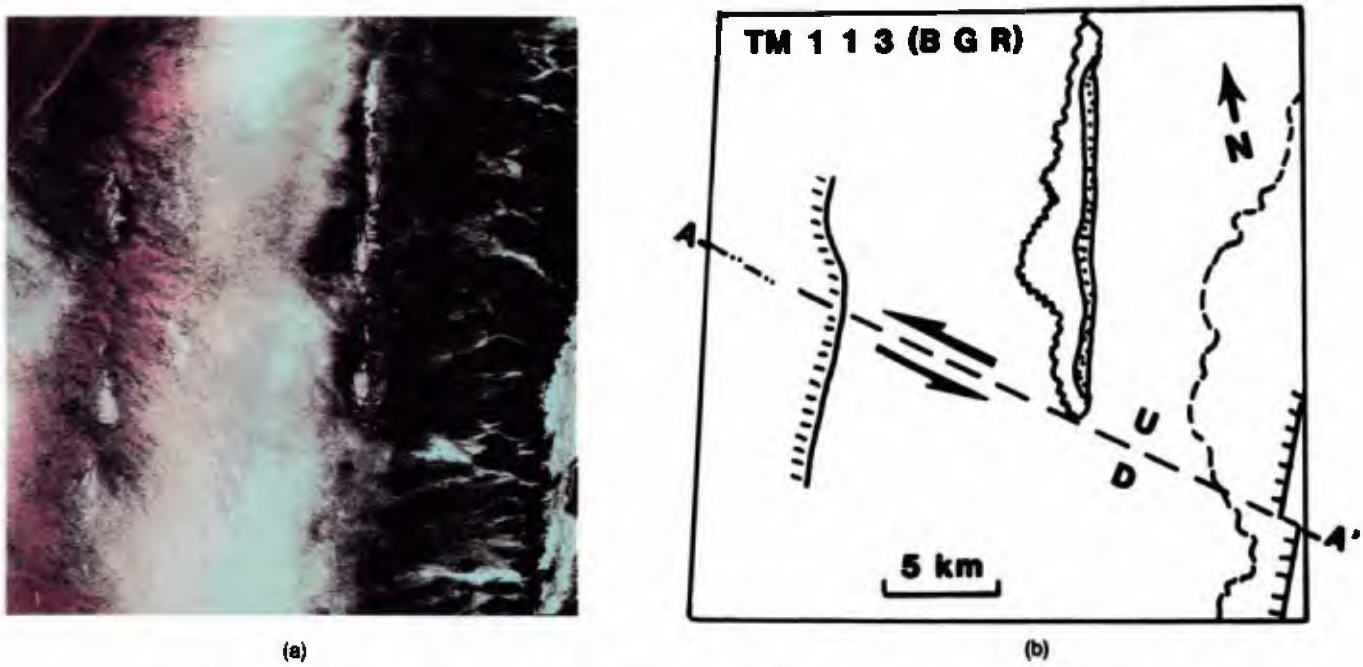

PLATE 1. (a) TM image (Subscene 1 on Figure 3) combines bands 1 (blue) and 3 (red) so that high iron oxide concentration will appear in red tones. The area shown is mostly sands and gravels on the west side of the Interior Homocline. (b) Interpretive sketch of the features mapped from Plate 1a.

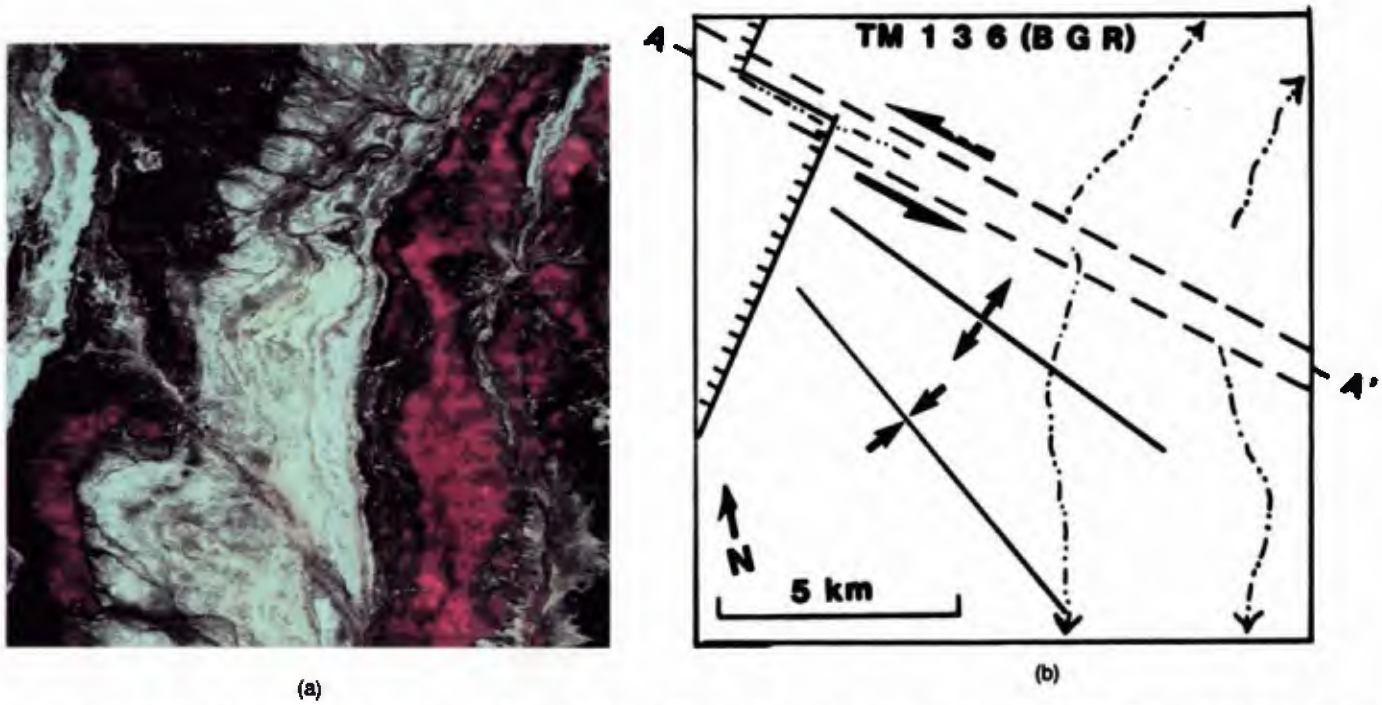

PLATE 2. (a) TM image (Subscene 2 on Figure 3) combining bands 1, 3, and 6 (Table 1). The thermal band (red) is affected by slope and physical properties; high iron oxide concentration in wadi channels, green; oldest strata on west side, dark blue. (b) Interpretive sketch of the features mapped from Plate 2a.

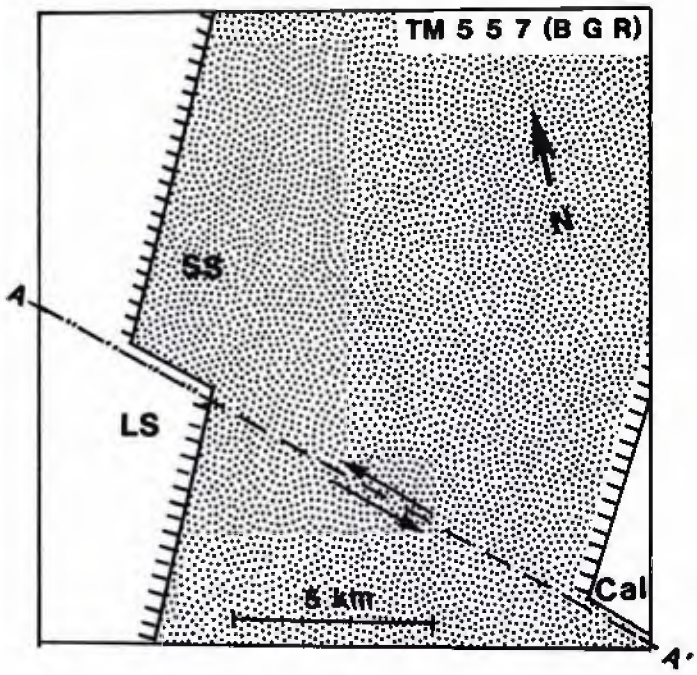

(a) (b)

PLATE 3. (a) TM image (Subscene 4 on Figure 3) combining visible and near-IR bands 5 and 7 to distinguish limestones (blue) from sandstones (red) in Cretaceous units. A road runs north-south near the center of the image. (b) Interpretation sketch. The juxtaposition of calcareous and sandstone lithofacies indicates left-lateral offset along A – A'.

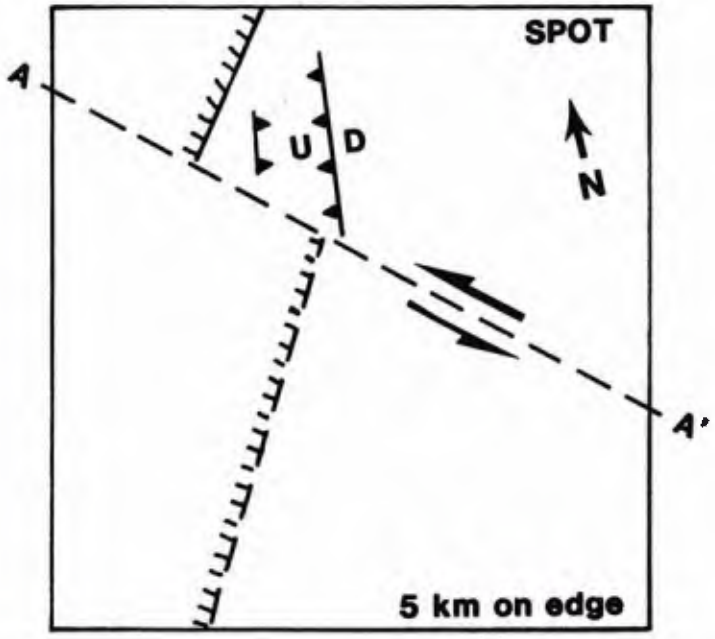

(a) (b)

PLATE 4. (a) High-resolution SPOT image of the Cretaceous-age promontory in the southeast corner of Plate 3. (b) Interpretation sketch. The two parallel features north of A – A' form an angle of about 55 degrees with the reference line and trend approximately north-south. The offset of the cuesta scarp is about 2.5 km. SPOT image Copyright 1987 CNES.

shows the resemblance to thrust faults that develop normal to the direction of maximum contraction (Figure 4).

SUMMARY AND DISCUSSION

Regional and local evidence of unmapped Najd faults in late-Paleozoic and Mesozoic outcrops has been presented. The broad view in AVHRR thermal-IR images shows three major subparallel extensions of the Najd Zone into Tertiary outcrops. The one discussed in this paper appears to separate fault blocks for a distance of more than 100 km because, from one side of the fault to the other, (1) the direction of drainage changes; (2) the strikes of the parallel scarps intersected shift by 10°, and (3) scarps are offset in a left-lateral sense.

Locally, topographic and lithologic features in TM and SPOT subscenes indicate offsets, *en echelon* folds, and secondary faults of a left-lateral "simple" shear system. Evidence of a fault trending N55°W can be seen in Permian to Cretaceous outcrops. In the AVHRR thermal-IR image, it can be traced to Tertiary outcrops beyond the eastern limits to the TM scene (Andre and Blodget, 1984).

The throughgoing fault in the Phanerozoic cover is unusually long and straight compared to the braided Najd faults in the Shield. However, lateral discontinuities from a patchwork of metamorphic, volcanic, and igneous intrusive units produced in the Shield during different stress regimes can deflect faults. A simpler fault pattern may result in sedimentary strata that are laterally homogeneous. On the other hand, there may be some braiding that cannot be detected because of the spatial resolution limitations of the data sets.

En echelon folds generally develop in relatively weaker or softer beds and also in the relatively more active fault block. Because the lithology of the north-south trending cuestas is homogeneous both north and south of the fault, the folds interpreted from these data would indicate that the southern block is the more active one.

In an independent study, Moore (1983) came to the same conclusion reached here based on the TM and SPOT data: the Najd Fault System is far longer than previously thought. From aeromagnetic data, he inferred a 70-km long fault in the crystalline Shield that is close to the orientation and alignment of the fault in Phanerozoic outcrops discussed here. The magnetic features correlate with mafic and ultramafic dikes that intruded along fault planes formed in an extensional environment toward the end of the Najd faulting in the early Cambrian. Moore reported that individual strands of the Najd fault system south of latitude 21°N have sinistral displacement of a few kilometres and that their combined offset may exceed 100 km. The aeromagnetic maps indicate that the Najd Belt is broader at depth than at the outcropping fault complex, and that more continuous structures underlie the surface faults (Moore, 1979).

Reactivation of the Najd Fault System could be related to uplift (locally as much as 5 km) in a belt that extends up to 500 km inland and postdates rifting of the Red Sea (Bohannon, 1988). However, east-west compressive stress within the Plate, as a result of expansion in the Red Sea and collision with the Eurasian Plate would be more likely to cause northwest-trending left-lateral faulting (Figure 4). The optimum primary direction of shortening for reactivating faults of the Najd (N45°W to N55°W) is N75°W to N85°W. This direction is also nearly optimum for buckling of the Rub al Khali basin in the Tertiary, the direction of foreshortening, normal to its northnortheast axis (Figure 1).

If the Najd Fault System extends to the Arabian interior and can be extrapolated beneath sands of the Empty Quarter to meet like-trending faults in South Yemen, the fault system would connect opposite boundaries of the Arabian Plate. Furthermore, if left-lateral fault extensions into the Eastern Desert of Egypt (Sultan *et al.*, 1988) and the Arabian Sea floor (Brown, 1972 are considered, the total length would exceed 3000 km.

ACKNOWLEDGMENTS

This research was supported by NASA grant NAGW-958. My thanks to Herb Blodget, Mohammed Sultan, Bob Stern, and Glen Brown for their helpful comments on the content of this paper. My thanks also go to Norman Hubbard and Pat Jacobberger for their suggestions for improving the manuscript and to Linda King at the National Air and Space Museum for her drafting help. Only I can be held responsible for the interpretations.

REFERENCES

American Society of Photogrammetry, 1983. *Manual of Remote Sensing* American Society of Photogrammetry, Falls Church, Virginia, 2440 p.

Andre, C. G., 1987. Geologic applications of SPOT-1, TM and NOAA-7 data; finding and defining unmapped structural features, *SPOT-1 Image Utilization, Assessment, Results*, Paris, France, pp. 837–844.

Andre, C. G., and H. W. Blodget, 1984. Thermal infrared satellite data for the study of tectonic features, GRL, 11, 983–986.

Armijo R., P. Tapponnier, J. L. Mercier, and H. Hong-Lin, 1986. Quaternary extensions in southern Tibet: field observations and tectonic implications, *JGR* 91, 13803–13872.

Bohannon, R. G., 1986. Tectonic configuration of the western Arabian continental margin, southern Red Sea, *Tectonics* 5, pp. 477–499.

Brown, G. F., 1972. *Tectonic Map of the Arabian Peninsula*, scale: 1:4,000,000, Min. of Petrol. and Min. Res., Dir. Gen of Min. Res. Kingdom of Saudi Arabia, Arabian Peninsula Series, Map AP-2.

Bramkamp, R. A., R. D. Gierhart, G. F. Brown, and R. O. Jackson, 1956. *Geology of the Southern Najd Quadrangle, Kingdom of Saudi Arabia*, scale 1:500,000, USGS Invest. Map I 212A, U. S. Geol. Surv.

Freund, R., Z. Garfunkel, I. Zak, M. Goldberg, T. Weissbrod, and B. Derin, 1970. The shear along the Dead Sea rift, *Phil. Trans. Roy. Soc. Lond.* A. 267, 107–130.

Gettings, M. E., H. R. Blank, W. D. Mooney, and J. H. Healey (1986). Crustal structure of southwestern Saudi Arabia, *JGR* 91, 6491–6512.

Harding, T. P., 1976. Tectonic significance and hydrocarbon trapping consequences of sequential folding synchronous with San Andreas faulting, San Joaquin Valley, California. *Amer. Assoc. Petrol. Geol. Bul.*, 60, 356–378.

Moody, J. D., and M. J. Hill, 1956. Wrench-fault tectonics, *Bull. GSA*, 67, 1207–1246.

Moore, J., 1979. Tectonics of the Najd Transcurrent Fault System, Saudi Arabia, *J. geol Soc. London*, 136, 441–454.

———, 1983. *Tectonic Fabric and Structural Control of Mineralization in the Southern Arabian Shield: A Compilation Based on Satellite Imagery Interpretation*, Open File Report USGS-OF-03-105.

Moore, J., and A. M. Al-Shanti, 1979. Structure and mineralization in the Najd Fault System, Saudi Arabia. Evolution and Mineralization of the Arabian/Nubian Shield, *I.A.G. Bul.*, 3, Pergamon Press, New York.

Phillips, L. F., and S. A. Schumm, 1987. Effect of regional slope on drainage networks, *Geology* 15, 813–816.

Powers, R. W., L. F. Ramirez, C. D. Redmond, and E. L. Elberg, Jr., 1966. *Geology of the Arabian Peninsula . Sedimentary Geology of Saudi Arabia*, USGS P-560-D.

Quennell, A. M., 1958. The structural geomorphic evolution of the Dead Sea rift. *Q. J. Geol. Soc. London* 114, 1–24.

Stern, R. J., 1985. The Najd fault system, Saudi Arabia and Egypt: A late preCambrian rift-related system? *Tectonics* 4, 497–511.

Stoesser, D. B., and V. E. Camp, 1985. Pan-African microplate accretion of the Arabian Shield: *GSA Bul.*, 96, 817–826.

Sultan, M., R. E. Arvidson, I. J. Duncan, R. J. Stern, and Baher El Kaliouby, 1988. Extension of the Najd shear system from Saudi Arabia to the Central Eastern Desert of Egypt based on integrated field and Landsat observations, *Tectonics* 7, 1291–1306.

Sylvester, A. G., 1988. Strike-slip faults, *GSA Bull.* 100, 1666–1703.

Tchalenko, J. S., 1970. Similarities between shear zones of different magnitudes, *GSA Bull.* 81, 1625–1640.

Wilcox, R. E., T. P. Harding, and D. R. Seely, 1970. Basic wrench tectonics, *AAPG 57*, 74–96.